Bond Theory

DOI: 10.1002/anie.201305505

Disentanglement of Donation and Back-Donation Effects on Experimental Observables: A Case Study of Gold–Ethyne Complexes**

Giovanni Bistoni, Leonardo Belpassi, and Francesco Tarantelli**

The Dewar–Chatt–Duncanson (DCD) model[1–3] was introduced more than 60 years ago to describe the η^2 coordination of ethene to a coinage-metal atom. It gives a formally simple picture of the bond between an unsaturated substrate (S) and a transition metal (M), which involves the donation of π electrons from the substrate to empty dσ orbitals of the metal ($S \rightarrow M$) and the back donation from filled dπ orbitals of the metal to empty substrate orbitals of the proper symmetry ($M \rightarrow S$). In unsaturated organic systems, these empty orbitals have typically a π^* anti-bonding character and their population tends to weaken the C–C bond, but a reverse effect may also be observed if the empty orbitals have a bonding character, as recently observed.[4–6] The DCD model enjoys enormous popularity among chemists, as it represents the standard framework in which to analyze the electronic properties of ligands and metal fragments, especially with a view of rationalizing and controlling the activation of substrates in catalyzed chemical reactions. It appears also appropriate for the captodative description of the carbon bond.[7]

Despite the fact that the DCD model is so well accepted, the assessment of the relative importance of the donation and back-donation contributions to the bond is often ambiguous and controversial.[8–13] The components of the DCD model are quantum-mechanically not well defined[14] and, while conclusions are commonly drawn from indirect experimental clues, they may be unreliable because no rigorous quantitative relationship, of either theoretical or empirical nature, has ever been established between observed properties and the DCD bond components. In fact, even just proving that the relative extent of donation and back donation can at all be extracted from experiments would be a highly desirable feat. Herein, we demonstrate that the DCD components can be effectively disentangled, and in principle quantitatively revealed, by measuring simple experimental observables. As a prototype case study we consider the bond between gold and ethyne. Such coordination systems have received increasing attention in the recent impetuous development of novel homogeneous-phase catalytic systems for alkyne activation.[15–19] Our analysis, which builds on a clear-cut quantitative definition of the DCD components, aims, at first, to show how donation and back donation in $[\mathrm{Au_3}\text{–ethyne}]^+$ correlate with simple observables, the bending of the C–C–H moiety and the redshift of the C–C stretching frequency of ethyne. Having established this correlation, we then show that it is surprisingly accurate for a large number of compounds in which ethyne interacts with other metal substrates.

As mentioned above, the key component of our analysis is a satisfactory and objective definition of the donation and back-donation charges. This can be obtained starting from the charge-displacement function (CDF):[20]

$$\Delta q(z) = \int_{-\infty}^{z} dz' \int_{-\infty}^{\infty} \int_{-\infty}^{\infty} \Delta\rho(x,y,z')dxdy \qquad (1)$$

where $\Delta\rho$ is the difference between the electron density of a complex and that of its non-interacting fragments (ethyne and the metal substrate, in our case), and z is any suitable axis joining them. The CDF is the exact definition of the amount of electronic charge which, upon formation of the complex, is displaced from left to right (the direction of decreasing z) across the plane perpendicular to the axis at point z. As previously demonstrated,[21,22] for suitably symmetric complexes and fragments, $\Delta\rho$, and consequently $\Delta q(z)$, can be decomposed into additive symmetry components which can be readily identified with the DCD components of the bond. In the present case, in order to separate the components, it is sufficient that the complex presents a symmetry plane perpendicular to the C–C bond of ethyne through its midpoint. All systems considered in this work have this C_s symmetry. In all cases, the z axis has been chosen as that joining the C–C midpoint of ethyne and the nearest metal atom. Geometries, harmonic frequencies, and electron densities were calculated using density functional theory including relativistic effects, as detailed in the Supporting Information. There, it is also shown that the CDFs are at convergence with respect to the basis set, relativistic effects, and the exchange-correlation functional employed.

As an example, Figure 1 presents the CDFs for the system $[\mathrm{Au_3}\text{–}\eta^2\text{ethyne}]^+$.[23] They clearly depict two charge fluxes moving in opposite directions across the whole molecular space, in the expected correspondence with their respective symmetry. The curve for the a′ symmetry, which correlates with the filled in-plane and out-of-plane π orbitals of ethyne, is everywhere positive, describing a net displacement of

---

[*] G. Bistoni, Dr. L. Belpassi, Prof. F. Tarantelli
Istituto di Scienze e Tecnologie Molecolari del CNR (CNR-ISTM)
Via Elce di Sotto 8, 06123 Perugia (Italy)
E-mail: leonardo.belpassi@cnr.it
G. Bistoni, Prof. F. Tarantelli
Dipartimento di Chimica, Biologia e Biotecnologie
Università di Perugia (Italy)
E-mail: franc@thch.unipg.it

[**] We acknowledge financial support from MIUR Italy through the "FIRB-Futuro in ricerca" (RBFR1022UQ) programme and thank D. Zuccaccia (Udine, Italy) for insightful discussions.

Supporting information for this article is available on the WWW under http://dx.doi.org/10.1002/anie.201305505.

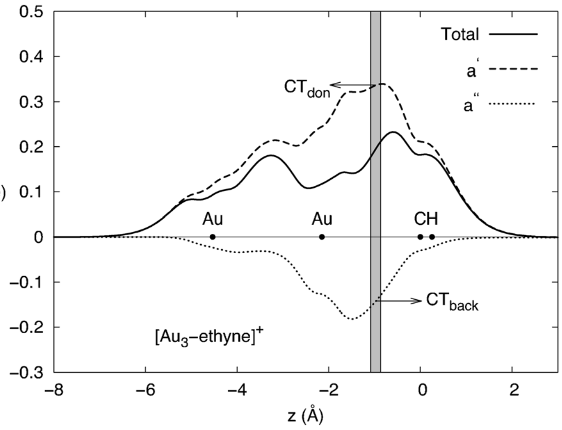

Figure 1. Charge displacement functions for the complex $[Au_3–\eta^2–ethyne]^+$. The dots on the axis mark the *z* coordinate of the atoms. The vertical band marks the isodensity boundary between the Au_3^+ and ethyne fragments (see text for details).

electrons in the direction from the alkyne toward the metal fragment (S→M donation). By contrast, the CDF for the a″ symmetry, correlating with the empty in-plane and out-of-plane π* ethyne orbitals, is negative in the whole bond region and thus describes a charge flux in the opposite direction (M→S back donation). Because donation is everywhere larger in magnitude than back donation, a net donation results, displayed as the total CDF. A reasonable measure of the charge transfer (CT) between ethyne and the Au_3^+ moiety can be obtained from the CDFs by fixing a plausible boundary plane between the fragments. Our standard choice is the *z* point where equal-valued isodensity surfaces of the isolated fragments become tangent. (The vertical band in Figure 1 marks a zone with a width of about one tenth of the Au–alkyne distance around this "isodensity boundary".) Across this boundary, the net CT from ethyne to Au_3^+ is 0.19 electrons, resulting from a donation of 0.33 electrons (CT_{don}) and a back donation of 0.14 electrons (CT_{back}). The CDFs thus give us a clear-cut, spatially detailed picture of the coordination bond and a plausible, unambiguous measure of the DCD components. The question we wish to address now is: is there a demonstrable relationship between these DCD components of the bond and experimental observables?

It is almost invariably observed that, upon binding to a metal fragment, ethyne undergoes a measurable distortion from linearity, $\Delta\theta$, and a decrease of the symmetric C–C stretching frequency, $\Delta\nu$. We keep our model as simple as possible and suppose that these quantities correlate linearly with the magnitude of CT_{don} and CT_{back}, according to the following expressions:

$$\begin{aligned}\Delta\theta &= a_1|CT_{\rm don}| + a_2|CT_{\rm back}| + \Delta\theta_{\rm elect}\\ \Delta\nu &= b_1|CT_{\rm don}| + b_2|CT_{\rm back}| + \Delta\nu_{\rm elect}\end{aligned} \tag{2}$$

In each equation, in order to take into account the effect of the electrostatic contribution, which is unknown and potentially large especially for charged systems, we added an additional term, $\Delta\theta_{elect}$ and $\Delta\nu_{elect}$, respectively. a_1, a_2, b_1, and b_2 are coefficients to be determined. In order to estimate these, we have calculated the dependence of all quantities in Equations (2) on the distance *r* between the C–C midpoint and the nearest gold atom of Au_3^+. At each distance, the structure of ethyne has been fully optimized within the C_s symmetry constraint. The results are summarized in Figure 2. In panel (a), we report the *r* dependence of the DCD components extracted from our CDFs at the isodensity boundary. Clearly, the absolute values of CT_{don} and CT_{back} decrease as *r* increases and, as should be expected, the data are perfectly described by exponential functions. The best fit yields $CT_{don}(r) = 1.6e^{-0.74r}$ and $CT_{back}(r) = -155.6e^{-3.25r}$ (with *r* in angstrom and CT in electrons). The difference in the rate of decay of the two components, with back donation falling off significantly faster, leads to a net CT function that presents a maximum at a distance of 2.5 Å (i.e. 0.4 Å larger than the equilibrium distance).

The *r* dependence of the reference observables $\Delta\theta$ and $\Delta\nu$ are reported in panels (b) and (c), respectively, together with the electrostatic contributions. The latter have been estimated by computing distortion and frequency of an ethyne molecule placed in the field of three point charges replacing the Au atoms, of value equal to the computed Au atomic charges in the Au_3–ethyne adduct. (As shown in the Supporting Information, the results are essentially identical with various methods to compute these charges.) The electrostatic contributions present a smooth *r* dependence that is well fitted by simple polynomials. The best-fit functions $CT_{don}(r)$ and $CT_{back}(r)$ of Figure 2a, together with the electrostatic terms, are used in Equations (2) to determine the constants a_1, a_2, b_1, and b_2, by fitting the *r* dependence of the reference observables.

Given the simplicity of the model adopted, the accuracy of the fit over a wide distance range is remarkable (see Figure 2). The calculated constants for $\Delta\theta$ are $a_1 = 7.9$ degrees/electron and $a_2 = 57.5$ degrees/electron, which clearly show that distortion is largely dominated by the effect of the back donation. In fact, it will not escape the reader's notice that a_2 is very close to the 60 degrees/electron one would theoretically expect for the full rehybridization of the carbon atoms from sp to sp^2.[24] At the equilibrium distance, the donation and back donation components account for 20% and 57% of the ethyne bending, respectively, while the electrostatic contribution is 23%. The C–C frequency redshift is also predominantly influenced by back donation but here the donation contribution is relatively more pronounced. The computed b_1 and b_2 constants are 193 cm^{-1}/electron and 528 cm^{-1}/electron, respectively, so that, at the equilibrium distance, the donation and back-donation components contribute nearly equally (42% and 53%, respectively), while the electrostatic term is only a small correction (less than 5%).

As a final independent check of the correlations just presented, we tested the ability of Equations (2), with the constants found above, to predict distortion and redshift of ethyne bound to several systems, including fourteen charged (+1) gold clusters (up to Au_{15}, and considering various isomers and coordination sites) and a number of charged and neutral $L–Au^I$ fragments, with the ligand L ranging from simple phosphines (PH_3, PF_3) to the N-heterocyclic carbene (NHC) 2,3-dihydroimidazol-2-ylidene, the chloride ion Cl^-,

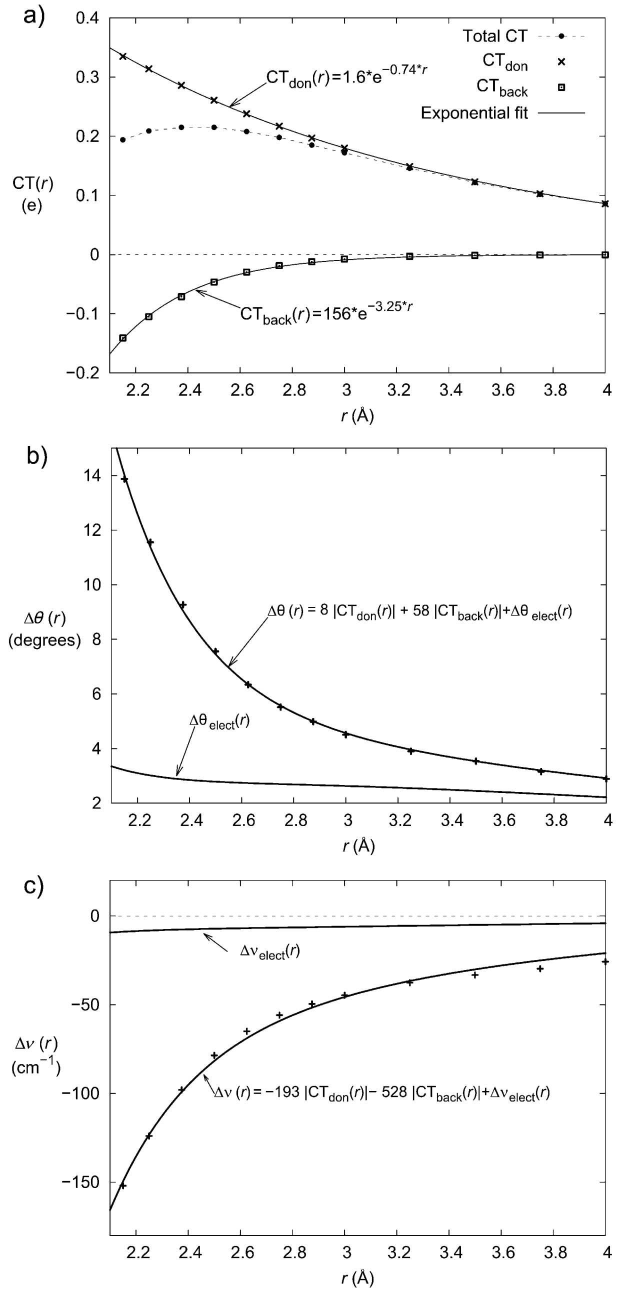

Figure 2. a) Dependence of the donation and back-donation charges and net CT on the distance r between Au_3^+ and ethyne. Shown are the computed points and the exponential best-fit lines. b) Distortion $\Delta\theta$ of ethyne from linearity as a function of its distance r from Au_3^+. Shown are the reference computed points, the best-fit line according to Equations (2), and the electrostatic contribution $\Delta\theta_{elect}$. c) C–C stretching frequency shift $\Delta\nu$ of ethyne as a function of its distance r from Au_3^+. Shown are the reference computed points, the best-fit line according to Equations (2) and the electrostatic contribution $\Delta\nu_{elect}$.

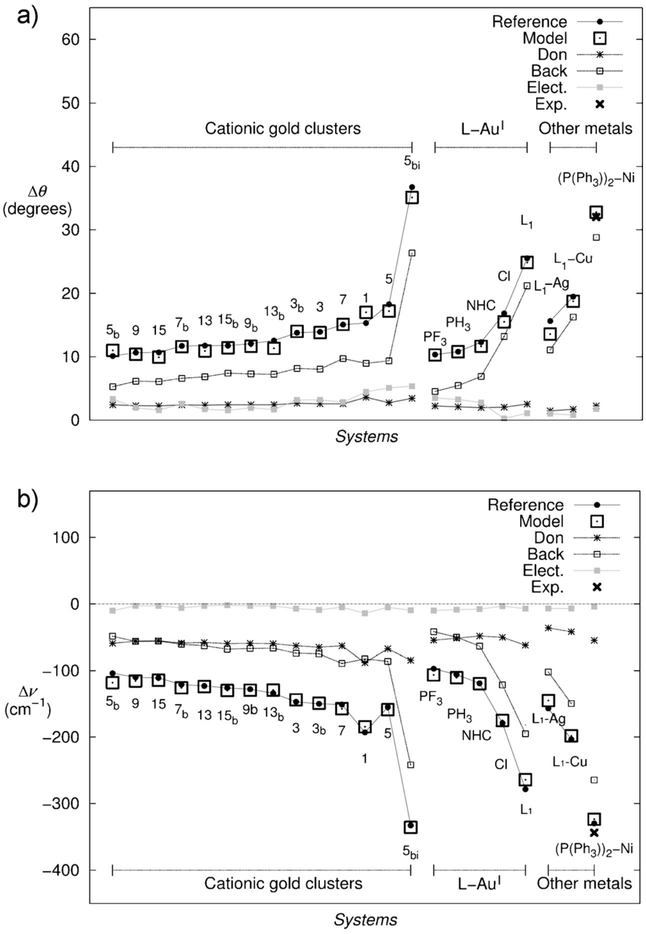

Figure 3. Reference and predicted (model) ethyne distortion (a) and frequency shift (b) in various chemical compounds (see the text and Supporting Information for details). The individual donation, back-donation, and electrostatic contributions appearing in Equation (2) are also shown. The crosses indicate experimental values. The stretching frequency of free ethyne in the gas phase is 1974 cm^{-1}.[37]

and a triazapentadienil ligand $[N\{(CF_3)C(Ph)N\}_2]$ (L_1). These complexes are closely related to recent gold(I)–alkyne intermediates characterized experimentally.[25–31] Moreover, we also included some examples of ethyne bound to different metals: the isoleptic systems L_1–Ag^+ and L_1–Cu^+, and $(P(Ph)_3)_2$–Ni. The results are summarized in Figure 3. The Supporting Information contains all the calculation details and we only note here that the computed distortions of ethyne from linearity in L–Au^I are entirely consistent with available X-ray crystallographic structures of analogous complexes of gold(I) with simple alkynes (see Ref. [25] and references therein). In the case of the Ni complex, the available experimental data of Ref. [32], shown in the figure, compare very well with the calculations.

The systems examined present a large variability in terms of the nature of the metal–ethyne interaction, with a binding energy spread of about 40 Kcal mol^{-1} and a CT_{don}/CT_{back} ratio going from 3.6 of $[PF_3$–Au–ethyne$]^+$ to 0.6 in the Ni complex. In view of this, the predictive accuracy of our model (see Figure 3) is impressive. The example of $[Au_5$–ethyne$]^+$ stands out as especially interesting in this respect: the three isomers labeled 5_b, 5, and 5_{bi} in the figure, differing as to cluster conformation and/or site of approach of ethyne, display CT_{don}/CT_{back} ratios of 3.3, 2.4, and 0.9, respectively, and this variability is clearly reflected in the observables under analysis. Such wide modulation of the bond nature and properties in a single system may be of great relevance for catalytic activity in the homogeneous phase, as shown recently for small gold clusters.[33–35]

The different contributions of Equations (2) are also displayed in the figure and clearly indicate that the dominating source of variability among the various systems is the back-donation component, while the donation and electrostatic terms remain relatively more stable. There is however a significant difference in the relative magnitude of the contributions to the two observables. The donation and electrostatic components play a relatively small and comparable role in ethyne distortion, while the magnitude of the donation contribution to the frequency shift is much larger, the electrostatic term being almost negligible in this case.

The importance of the results shown in Figure 3 for one of the most popular chemical-bond models and for coordination chemistry in general can hardly be overestimated. Besides proving the consistency and robustness, as well as the transparent simplicity, of the charge-displacement analysis, they demonstrate for the first time the existence of a quantitative relationship between measurable properties and the DCD bond constituents. Through suitable experiments, these may therefore be disentangled and crucial insight into the nature of coordination bonds may thus be gained. It might be possible and relevant, for example, to identify observables which selectively depend on a specific bond component,[36] and the charge-displacement analysis clearly suggests itself as a helpful tool to achieve this goal.

Received: June 26, 2013

Keywords: alkyne ligands · bond theory · density functional calculations · gold · multiple bonds

---

[1] M. J. S. Dewar, *Bull. Soc. Chim. Fr.* **1951**, *18*, C71–C79.
[2] J. Chatt, L. A. Duncanson, *J. Chem. Soc.* **1953**, 2939–2947.
[3] G. A. Gamlen, J. Lewis, D. M. Adams, J. R. Postgate, R. G. Pearson, F. Basalo, R. B. H. Crabtree, T. Ito, B. Chaudret, H. W. Fruhauf, B. T. Heaton, J. S. McIndoe, J. R. Sanders, C. Floriani, T. S. A. Hor, M. Abou Rida, S. Otto, S. C. Lee, J. R. Harper, F. Dumitru, M. Hidai, D. M. P. Mingos, M. D. Fryzuk, C. A. N. McAuliffe, V. C. Gibson, A. Wedd, A. Roodt, L. A. Duncanson, R. G. Wilkins, J. R. Dilworth, C. D. Garner, G. Frenking, R. L. Richards, *Modern Coordination Chemistry: The Legacy of Joseph Chatt* (Eds.: N. Winterton, J. Leigh), The Royal Society of Chemistry, London, **2002**.
[4] H. Braunschweig, A. Damme, R. D. Dewhurst, A. Vargas, *Nat. Chem.* **2012**, *5*, 115–121.
[5] G. Frenking, N. Holzmann, *Science* **2012**, *336*, 1394–1395.
[6] H. Braunschweig, R. D. Dewhurst, K. Hammond, J. Mies, K. Radacki, A. Vargas, *Science* **2012**, *336*, 1420–1422.
[7] M. Alcarazo, C. W. Lehmann, A. Anoop, W. Thiel, A. Fürstner, *Nat. Chem.* **2009**, *1*, 295–301.
[8] A. M. Echavarren, *Nat. Chem.* **2009**, *1*, 431–433.
[9] I. Krossing, *Angew. Chem.* **2011**, *123*, 11781–11783; *Angew. Chem. Int. Ed.* **2011**, *50*, 11576–11578.
[10] A. Fürstner, L. Morency, *Angew. Chem.* **2008**, *120*, 5108–5111; *Angew. Chem. Int. Ed.* **2008**, *47*, 5030–5033.
[11] A. Fürstner, *Chem. Soc. Rev.* **2009**, *38*, 3208–3221.
[12] D. Benitez, N. D. Shapiro, E. Tkatchouk, Y. Wang, W. A. Goddard, F. D. Toste, *Nat. Chem.* **2009**, *1*, 482–486.
[13] M. M. Hansmann, F. Rominger, A. S. K. Hashmi, *Chem. Sci.* **2013**, *4*, 1552–1559.
[14] G. Frenking, N. Fröhlich, *Chem. Rev.* **2000**, *100*, 717–774.
[15] G. Hutchings, *Top. Catal.* **2008**, *48*, 55–59, 10.1007s11244-008-9048-5.
[16] Z. Li, C. Brouwer, C. He, *Chem. Rev.* **2008**, *108*, 3239–3265, PMID: 18613729.
[17] A. S. K. Hashmi, G. J. Hutchings, *Angew. Chem.* **2006**, *118*, 8064–8105; *Angew. Chem. Int. Ed.* **2006**, *45*, 7896–7936.
[18] N. T. Patil, *ChemCatChem* **2011**, *3*, 1121–1125.
[19] A. Corma, H. Garcia, *Chem. Soc. Rev.* **2008**, *37*, 2096–2126.
[20] L. Belpassi, I. Infante, F. Tarantelli, L. Visscher, *J. Am. Chem. Soc.* **2008**, *130*, 1048–1060.
[21] N. Salvi, L. Belpassi, F. Tarantelli, *Chem. Eur. J.* **2010**, *16*, 7231–7240.
[22] D. Zuccaccia, L. Belpassi, F. Tarantelli, A. Macchioni, *Eur. J. Inorg. Chem.* **2013**, *24*, 4121–4135.
[23] Ligand stabilized tri-gold cation has been recently synthesized. See: T. J. Robilotto, J. Bacsa, T. G. Gray, J. P. Sadighi, *Angew. Chem.* **2012**, *124*, 12243–12246; *Angew. Chem. Int. Ed.* **2012**, *51*, 12077–12080.
[24] R. H. Crabtree, *The Organometallic Chemistry of the Transition Metals*, 4th ed., Wiley, Hoboken, **2005**.
[25] H. G. Raubenheimer, H. Schmidbaur, *S. Afr. J. Sci.* **2011**, *107*, 01–13.
[26] H. Schmidbaur, A. Schier, *Organometallics* **2010**, *29*, 2–23.
[27] T. N. Hooper, M. Green, C. A. Russell, *Chem. Commun.* **2010**, *46*, 2313–2315.
[28] N. D. Shapiro, F. D. Toste, *Proc. Natl. Acad. Sci. USA* **2008**, *105*, 2779–2782.
[29] H. V. R. Dias, J. A. Flores, J. Wu, P. Kroll, *J. Am. Chem. Soc.* **2009**, *131*, 11249–11255, PMID: 19610646.
[30] J. Wu, P. Kroll, H. V. R. Dias, *Inorg. Chem.* **2009**, *48*, 423–425.
[31] S. Flügge, A. Anoop, R. Goddard, W. Thiel, A. Fürstner, *Chem. Eur. J.* **2009**, *15*, 8558–8565.
[32] K. R. Pörschke, Y.-H. Tsay, C. Krüger, *Angew. Chem.* **1985**, *97*, 334–335; *Angew. Chem. Int. Ed. Engl.* **1985**, *24*, 323–324.
[33] J. Oliver-Meseguer, J. R. Cabrero-Antonino, I. Domínguez, A. Leyva-Pérez, A. Corma, *Science* **2012**, *338*, 1452–1455.
[34] A. S. K. Hashmi, *Science* **2012**, *338*, 1434.
[35] M. Boronat, A. Leyva-Pérez, A. Corma, *Acc. Chem. Res.* **2013**, DOI: 10.1021/ar400068w.
[36] O. Back, M. Henry-Ellinger, C. D. Martin, D. Martin, G. Bertrand, *Angew. Chem.* **2013**, *125*, 3011–3015; *Angew. Chem. Int. Ed.* **2013**, *52*, 2939–2943.
[37] K. Nakamoto, *Infrared and Raman Spectra of Inorganic and Coordination Compounds*, 6th ed., Wiley, Hoboken, **2009**.